

Kinetics and Mechanism of the Comproportionation of Hypothiocyanous Acid and Thiocyanate to Give Thiocyanogen in Acidic Aqueous Solution

Péter Nagy, Kelemu Lemma, and Michael T. Ashby*

Department of Chemistry and Biochemistry, University of Oklahoma, Norman, Oklahoma 73019

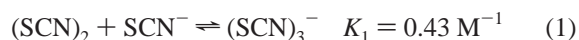
Received August 4, 2006

The kinetics of comproportionation of hypothiocyanous acid (HOSCN) and thiocyanate (SCN^-) to give thiocyanogen ($(\text{SCN})_2$) in acidic aqueous solutions have been determined by double-mixing stopped-flow UV spectroscopy. Hypothiocyanite (OSCN^-) was generated at pH 13 by oxidation of excess SCN^- with hypobromite (OBr^-), followed by a pH jump to acidic conditions ($[\text{H}^+] = 0.20\text{--}0.46\text{ M}$). The observed pseudo-first-order rate constants exhibit first-order dependencies on $[\text{H}^+]$ and $[\text{SCN}^-]$ with overall third-order kinetics. The corresponding kinetics of hydrolysis of $(\text{SCN})_2$ have also been examined. Under conditions of high (and constant) $[\text{H}^+]$ and $[\text{SCN}^-]$, the kinetics exhibit second-order behavior with respect to $[(\text{SCN})_2]$ and complex inverse dependences on $[\text{H}^+]$ and $[\text{SCN}^-]$. Under conditions of low $[\text{H}^+]$ and $[\text{SCN}^-]$, the kinetics exhibit first-order behavior with respect to $[(\text{SCN})_2]$ and independence with respect to $[\text{H}^+]$ and $[\text{SCN}^-]$. We attribute this behavior to a shift in the rate-limiting step from disproportionation of HOSCN (second-order dependency on $[(\text{SCN})_2]$) to rate-limiting hydrolysis (first-order dependency on $[(\text{SCN})_2]$). Thus, we have determined the following equilibrium constant by the kinetic method: $(\text{SCN})_2 + \text{H}_2\text{O} \rightleftharpoons \text{HOSCN} + \text{SCN}^- + \text{H}^+$; $K_{\text{hyd}} = [\text{HOSCN}][\text{SCN}^-][\text{H}^+]/[(\text{SCN})_2] = k_{\text{hyd}}/k_{\text{comp}} = 19.8(\pm 0.7)\text{ s}^{-1}/5.14(\pm 0.07) \times 10^3\text{ M}^{-2}\text{ s}^{-1} = 3.9 \times 10^{-3}\text{ M}^2$.

Introduction

Relatively little is known about the reaction chemistry of the human defense factor hypothiocyanite (OSCN^-),¹ in part because it is unstable, but also because until recently the only recognized means of preparing it has been the enzyme-catalyzed oxidation of SCN^- by H_2O_2 and hydrolysis of $(\text{SCN})_2$. The enzymatic process is limited to near-neutral pH, which is a condition for which OSCN^- is relatively unstable.² Early studies of OSCN^- have included hydrolysis of $(\text{SCN})_2$,³ a reaction that is usually initiated by the heterogeneous extraction of $(\text{SCN})_2$ from organic solvents (in which it was prepared by reaction of lead(II) thiocyanate with bromine) into aqueous solutions, a technique that is not conducive to studying fast reactions.^{4,5} Stanbury has recently investigated the aqueous chemistry of $(\text{SCN})_2$, which was generated under

very acidic conditions by oxidation of SCN^- .^{6–9} Stanbury's first studies of the oxidation of SCN^- by ClO_2 and H_2O_2 were hampered by the sluggish kinetics of the oxidation reactions and subsequent decomposition reactions of $(\text{SCN})_2$ that competed with its formation.^{7,8} This problem was overcome by employing Cl_2/HOCl as an oxidant mixture, which apparently produces $(\text{SCN})_2$ within the mixing time of a stopped-flow experiment.⁹ Stanbury's investigations have provided evidence that $(\text{SCN})_2$, in the presence of excess SCN^- , is in rapid equilibrium with trithiocyanate ($(\text{SCN})_3^-$) (cf. the corresponding equilibrium between I_2 and I_3^-):⁶



More recently, Stanbury et al. have investigated the decomposition of $(\text{SCN})_2$ under acidic conditions.⁹ These studies have yielded an equilibrium constant (K_2) for the hydrolysis of $(\text{SCN})_2$ to give hypothiocyanous acid (HOSCN) and SCN^- , as well as a rate constant for the disproportionation

* To whom correspondence should be addressed. E-mail: MAshby@ou.edu.

- (1) Ihalin, R.; Loimaranta, V.; Tenovuo, J. *Arch. Biochem. Biophys.* **2006**, *445*, 261–268.
- (2) Pruitt, K. M.; Tenovuo, J. O., Eds. *Immunology Series: The Lactoperoxidase System: Chemistry and Biological Significance*; Dekker: New York, 1985; Vol. 27, p 257.
- (3) Wood, J. L. *Org. React.* **1946**, *3*, 240–266.
- (4) Aune, T. M.; Thomas, E. L. *Eur. J. Biochem.* **1977**, *80*, 209–214.
- (5) Hoogendoorn, H.; Piessens, J. P.; Scholtes, W.; Stoddard, L. A. *Caries Res.* **1977**, *11*, 77–84.

- (6) Barnett, J. J.; Stanbury, D. M. *Inorg. Chem.* **2002**, *41*, 164–166.
- (7) Figlar, J. N.; Stanbury, D. M. *Inorg. Chem.* **2000**, *39*, 5089–5094.
- (8) Figlar, J. N.; Stanbury, D. M. *J. Phys. Chem. A* **1999**, *103*, 5732–5741.
- (9) Barnett, J. J.; McKee, M. L.; Stanbury, D. M. *Inorg. Chem.* **2004**, *43*, 5021–5033.

of HOSCN (k_3):



$$K_2 = \frac{k_2}{k_{-2}} = \frac{k_{\text{hyd}}^{\text{SCN}}}{k_{\text{comp}}^{\text{SCN}}} = 5.7 \times 10^{-4} \text{ M}^2 \quad (2)$$



$$k_3 = 6.9 \times 10^4 \text{ M}^{-1} \text{ s}^{-1} \quad (3)$$

We have recently investigated the kinetics of the reaction of hypochlorite (OCl^-)¹⁰ and hypobromite (OBr^-)¹¹ with SCN^- under alkaline conditions and learned that reactions between the corresponding hypohalous acids and SCN^- occur very fast and with near diffusion-controlled kinetics in the case of HOBr:



$$k(\text{X} = \text{Cl}) = 2.3 \times 10^7 \text{ M}^{-1} \text{ s}^{-1}, k(\text{X} = \text{Br}) = 2.3 \times 10^9 \text{ M}^{-1} \text{ s}^{-1} \quad (5)$$

In contrast to OCl^- , OBr^- also reacts with SCN^- with a measurable rate, albeit with a rate constant ($3.8 \times 10^4 \text{ M}^{-1} \text{ s}^{-1}$) that is 5 orders of magnitude smaller than that of its conjugate acid.¹¹ Through the comparison of time-resolved electronic spectra, time-resolved ¹³C NMR spectra, and time-resolved ¹⁵N NMR spectra, we have concluded that the enzyme system (lactoperoxidase/ $\text{H}_2\text{O}_2/\text{SCN}^-$), hydrolysis of $(\text{SCN})_2$, and oxidation of SCN^- by HOX ($\text{X} = \text{Cl}, \text{Br}$) all yield the same initial species.¹² The experimental^{12–17} and computed¹⁸ NMR shielding constants are consistent with a formulation of OSCN^- ,¹² and the NMR spectra appear to rule out alternative formulations of hypothiocyanite (e.g., OCNS^- , SOCN^- , ONCS^- , and OSNC^-).¹² The development of a facile in situ synthesis of OSCN^- by oxidation of SCN^- with OX^- ($\text{X} = \text{Cl}, \text{Br}$)^{10,11} affords the opportunity to investigate some of its chemical reactions, including the comproportionation of HOSCN with SCN^- ($k_{-2} = k_{\text{comp}}^{\text{SCN}}$, the reverse of eq 2), which we report here together with a reinvestigation of the hydrolysis of $(\text{SCN})_2$ that yields a direct measurement of the rate constant for eq 2 ($k_2 = k_{\text{hyd}}^{\text{SCN}}$).

Experimental Section

Reagents. All chemicals were ACS certified grade or better. Water was doubly distilled in glass. Solutions of NaOH, mostly free of CO_2 contamination, were quantified by titration with a

standardized HCl solution using phenolphthalein as an indicator. The buffer solutions were prepared from the solids $\text{NaH}_2\text{PO}_4 \cdot \text{H}_2\text{O}$, Na_2HPO_4 , and $\text{Na}_3\text{PO}_4 \cdot 12\text{H}_2\text{O}$, the ionic strength was adjusted with NaClO_4 , and the pH was adjusted with NaOH or HClO_4 . Stock solutions of NaSCN were prepared after drying in a 150 °C oven to constant weight. Stock solutions of NaOCl were prepared by sparging Cl_2 into a 0.3 M solution of NaOH. The sparging was stopped when the $[\text{OCl}^-]$ achieved ca. 100 mM, as determined spectrophotometrically ($\epsilon(\text{OCl}^-)_{292\text{nm}} = 350 \text{ M}^{-1} \text{ cm}^{-1}$). Solutions of NaOBr were prepared by adding Br_2 to ice-cold solutions of NaOH.¹⁹ Solutions of OBr^- were standardized spectrophotometrically at 329 nm ($\epsilon_{329} = 332 \text{ M}^{-1} \text{ cm}^{-1}$).¹⁹ The solutions of OCl^- and OBr^- were used within 2 h of the preparations to minimize errors due to decomposition.

UV/Visible Spectroscopy. Electronic spectra were measured using a HP 8452A diode-array spectrophotometer or the monochromator of a HI-TECH SF-61 DX2 stopped-flow instrument.

pH Measurements. The $[\text{OH}^-]$ for the unbuffered solutions was determined by acid–base titration against standardized HCl solutions. HClO_4 and HCl were standardized against bicarbonate. The $[\text{H}^+]$ of the buffered solutions were determined with an Orion Ion Analyzer EA920 using an Ag/AgCl combination pH electrode. The ionic strength was kept constant at 1.0 M for all solutions ($\text{NaClO}_4 + \text{HClO}_4 + \text{NaSCN} + \text{NaH}_2\text{PO}_4$). All pH measurements were corrected for the “Irving factor” of the working medium. A value of $\text{p}K_w$ of 13.79 was used for the $[\text{H}^+]$ or $[\text{OH}^-]$ calculations according to Martell and Smith.²⁰

General Description of the Stopped-Flow Studies. Kinetic measurements for the reaction of HOSCN with SCN^- and the hydrolysis of $(\text{SCN})_2$ were made with a HI-TECH SF-61 DX2 stopped-flow spectrophotometer using a Xe arc lamp and a PMT detector. A double-mixing mode was used for all of the experiments. All monochromatic traces were collected at $\lambda = 300 \text{ nm}$ using a 1 cm optical path length. During all of the stopped-flow measurements, a temperature of 291 K was maintained in the observation cell with a Lauda RC-20 circulator. The adiabatic temperature increases that were associated with the pH-jump experiments were determined experimentally to be less than 1 °C.

Calibration of the HI-TECH SF-61 DX2 Stopped-Flow Instrument. The instrument was calibrated in both single- and double-mixing modes using the reaction of 2,6-dichlorophenol-indophenol (DCIP) and ascorbic acid (AA) reaction at pH 1.80 under pseudo-first-order conditions (excess [AA]).²¹ The plot of [AA] vs k_{obs} started to deviate from linearity when k_{obs} was larger than 400 s^{-1} , indicating that the highest limit of k_{obs} that could be measured for a (pseudo) first-order reaction on our HI-TECH SF-61 DX2 stopped-flow instrument is 400 s^{-1} . The dead time and the pretriggering time of the instrument were determined on the basis of the following equations:

$$\text{Dead time: } A_{\text{obs}} = A_{\text{tot}} e^{-k_{\text{obs}} t_d}$$

$$\text{Pretriggering time: } A_{\text{tot}} = A_{\text{fit}} e^{-k_{\text{obs}} t_s}$$

where A_{obs} is the observed absorbance maximum; A_{tot} is the effective absorbance change associated with the reaction; A_{fit} is the fitted absorbance change (extrapolated to $t = 0$); t_d is the dead time; and t_s is the pretriggering time of the instrument. It has been previously

(10) Ashby, M. T.; Carlson, A. C.; Scott, M. J. *J. Am. Chem. Soc.* **2004**, *126*, 15976–15977.

(11) Nagy, P.; Beal, J. L.; Ashby, M. T. *Chem. Res. Toxicol.* **2006**, *19*, 587–593.

(12) Nagy, P.; Alguindigue, S. S.; Ashby, M. T. *Biochem.* **2006**, *45*, 12610–12616.

(13) Arlandson, M.; Decker, T.; Roongta, V. A.; Bonilla, L.; Mayo, K. H.; MacPherson, J. C.; Hazen, S. L.; Slungaard, A. *J. Biol. Chem.* **2001**, *276*, 215–24.

(14) Modi, S.; Behere, D. V.; Mitra, S. *Biochim. Biophys. Acta* **1991**, *1080*, 45–50.

(15) Modi, S.; Deodhar, S. S.; Behere, D. V.; Mitra, S. *Biochem.* **1991**, *30*, 118–124.

(16) Pollock, J. R.; Goff, H. M. *Biochim. Biophys. Acta* **1992**, *1159*, 279–85.

(17) Walker, J. V.; Butler, A. *Inorg. Chim. Acta* **1996**, *243*, 201–206.

(18) Sundholm, D. *J. Am. Chem. Soc.* **1995**, *117*, 11523–11528.

(19) Troy, R. C.; Margerum, D. W. *Inorg. Chem.* **1991**, *30*, 3538–43.

(20) Martell, A. E.; Smith, R. M. *Critical Stability Constants, Vol. 4: Inorganic Complexes*; Plenum Press: New York, 1976.

(21) Tonomura, B.; Nakatani, H.; Ohnishi, M.; Yamaguchi-Ito, J.; Hiromi, K. *Anal. Biochem.* **1978**, *84*, 370–83.

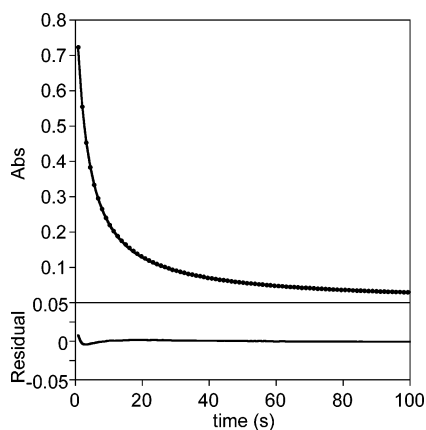


Figure 1. Time-absorbance trace at $\lambda = 300$ nm for the hydrolysis of thiocyanogen under relatively high $[\text{H}^+]$ and high $[\text{SCN}^-]$ (30% of the data points are illustrated). This measurement was achieved using a double-mixing stopped-flow sequence, where Cl_2 was generated in situ by mixing a solution of 20 mM HOCl (pH 7.91 in 1 M NaClO_4) and 0.93 M H^+ in the first mixing cycle, which results in a reaction mixture of 10 mM Cl_2 in 0.47 M H^+ ($I = 1$ M). This reaction mixture was then mixed with 100 mM SCN^- in 0.47 M H^+ ($I = 1$ M). The concentrations at $t = 0$ are $[(\text{SCN})_2]_0 = 5$ mM, $[\text{SCN}^-] = 40$ mM, $[\text{H}^+] = 0.47$ M, $I = 1$ M ($\text{NaClO}_4 + \text{HClO}_4 + \text{NaSCN}$). A homogeneous second-order fit is illustrated together with its residual.

shown mathematically that it is not necessary to correct for a concentration gradient within the stopped-flow observation cell for a (pseudo) first-order reaction (as opposed to fast second-order reactions, where the aging of the reaction mixture has to be taken into account and the observed rate constants has to be corrected using the geometrical parameters of the observation cell).²² We note that the effect of the mixing rate constant (k_{mix}) on k_{obs} was investigated, and we have found that no correction was necessary for the data collected with our instrument.

Reaction of HOSCN with SCN⁻. The H^+ and SCN^- concentration dependencies of the reaction rates were investigated under pseudo-first-order conditions with at least a 20-fold excess of SCN^- over HOSCN. The species OSCN^- was generated in situ by the reaction of SCN^- and OBr^- at pH 13 in the first mixing cycle¹¹ followed by a pH jump to the desired pH in the second mixing cycle. The following concentrations were achieved after the second mixing cycle:

Effect of $[\text{SCN}^-]$: $[\text{H}^+] = 0.46$ M; $[\text{OSCN}^-]_0 = 1.25$ mM;
 $[\text{SCN}^-] = 23.8\text{--}123.8$ mM

Effect of $[\text{H}^+]$: $[\text{SCN}^-] = 73.8$ mM; $[\text{OSCN}^-]_0 = 1.25$ mM;
 $[\text{H}^+] = 0.20\text{--}0.46$ M

We have previously reported that a 400-fold excess of SCN^- was required to produce stoichiometric amounts of OSCN^- with OCl^- at pH 13 when employing a Bio-Logic SFM-400/Q mixer.¹² We have determined that a 50-fold excess over OCl^- is required to produce >95% yield of HOSCN using the HI-TECH SF-61 DX2 stopped-flow instrument. Under similar conditions, OBr^- yields ~80% yield of HOSCN with the HI-TECH SF-61 DX2 stopped-flow instrument. For the pseudo-first-order conditions (excess SCN^- and constant $[\text{H}^+]$) that were employed in the present study, we have determined that the over-oxidation products do not influence the kinetics of the reaction of HOSCN with SCN^- .

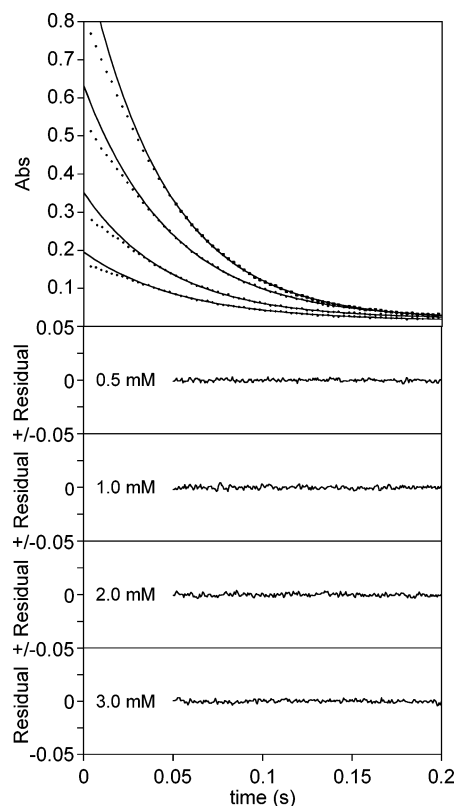


Figure 2. Time-absorbance traces at $\lambda = 300$ nm for the hydrolysis of thiocyanogen as a function of the $[(\text{SCN})_2]_0$ (0.5, 1.0, 2.0, and 3.0 mM) at pH 1.88 and $[\text{SCN}^-] = 0.1$ M (20% of the data points are illustrated). Equation 13 would be required to fit the entire absorption-time traces, but there are too many parameters in eq 13 to resolve them with the available data. However, the data can be modeled with single-exponential functions after the induction periods. First-order fits of the indicated portions of the data (solid lines) are illustrated together with their residuals. The rate constants that are computed for $[(\text{SCN})_2]_0 = 0.5\text{--}3.0$ mM are $18.4 (\pm 0.2)$, $20.9 (\pm 0.1)$, $20.42 (\pm 0.06)$, and $22.27 (\pm 0.04)$ s⁻¹, respectively.

Hydrolysis of (SCN)₂. The species $(\text{SCN})_2$ was generated in situ by the reaction of Cl_2/HOCl with excess SCN^- at $[\text{H}^+] = 0.2$ M in the first mixing cycle. The effects of $[\text{H}^+]$, $[\text{SCN}^-]$, and $[(\text{SCN})_2]_0$ on the reaction rates were investigated under pseudo-first-order conditions with at least a 25-fold excess of SCN^- over $(\text{SCN})_2$. A pH jump to the desired values in the second mixing cycle was achieved using a 0.2 M phosphate buffer of ca. pH 6. The following concentrations were achieved after the second mixing cycle:

Effect of $[\text{H}^+]$: $[\text{SCN}^-] = 0.10$ M; $[(\text{SCN})_2]_0 = 2.4$ mM;
 $[\text{H}^+] = 5.0\text{--}37.0$ mM.

Effect of $[\text{SCN}^-]$: $[\text{H}^+] = 12.9$ mM; $[(\text{SCN})_2]_0 = 2.0$ mM;
 $[\text{SCN}^-] = 50\text{--}130$ mM.

Effect of $[(\text{SCN})_2]_0$: $[\text{H}^+] = 13.2$ mM; $[\text{SCN}^-] = 0.10$ M;
 $[(\text{SCN})_2]_0 = 0.5\text{--}3.0$ mM.

Kinetic Data Analysis. The monochromatic kinetic traces were fit with HI-TECH KinetAsyst 3.14 software (Hi-Tech, UK). The concentration dependencies of the pseudo-first-order rate constants were obtained by linear least-squares fits of the data with Kaleida-Graph 3.6 (Synergy Software).

Results

Kinetics of Hydrolysis of Thiocyanogen. Our efforts to measure the kinetics of the hydrolysis of $(\text{SCN})_2$ by the initial

(22) Dunn, B. C.; Meagher, N. E.; Rorabacher, D. B. *J. Phys. Chem.* **1996**, *100*, 16925–16933.

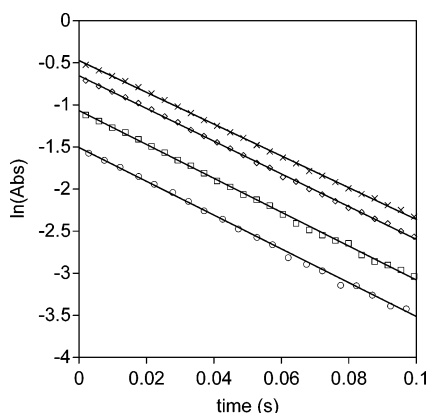


Figure 3. Change in absorption at $\lambda = 300$ nm (20% of the data illustrated) during the hydrolysis of $(\text{SCN})_2$ (2.0 mM) at pH 1.89 in the presence of 50 (○), 80 (□), 110 (◇), and 130 (×) mM SCN^- . Linear fits are illustrated with slopes of 20.2, 20.1, 19.3, and 18.8 s^{-1} for $[\text{SCN}^-] = 50, 80, 110,$ and 130 mM.

Table 1. Observed First-Order Rate Constants of the Hydrolysis of Thiocyanogen as a Function of pH

pH	$k_{\text{obs}} (\text{s}^{-1})^a$	pH	$k_{\text{obs}} (\text{s}^{-1})^a$
1.43	20.31 ± 0.06	1.84	23.80 ± 0.05
1.62	20.70 ± 0.06	2.30	27.37 ± 0.04

^a The estimated error is for a least-squares fit of an average of seven mixing cycles.

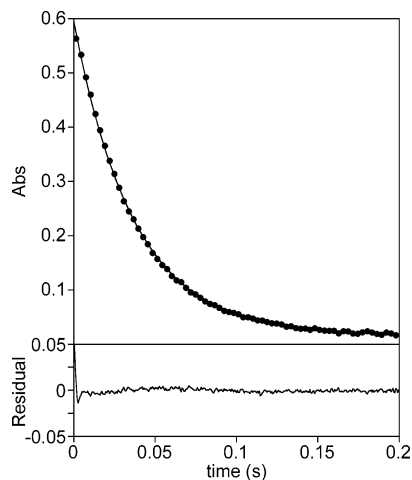


Figure 4. Time-absorbance traces at $\lambda = 300$ nm for the hydrolysis of thiocyanogen at pH 2.30 (30% of the data points are illustrated). Conditions: $[(\text{SCN})_2]_0 = 2.4$ mM, $[\text{SCN}^-] = 0.1$ M, $I = 1.0$ M. A first-order fit is illustrated together with its residual.

rate method for $[\text{H}^+] = 0.5$ M and $[\text{SCN}^-] = 0.1$ M were unsuccessful. The pseudo-zero-order rate constants exhibited a second-order dependency on $[(\text{SCN})_2]_0$ (unpublished results), which suggested that disproportionation of HOSCN is the rate-limiting step under such conditions. Second-order kinetics, as previously observed by Stanbury et al.,⁹ were confirmed for more acidic conditions by monitoring the entire reaction and fitting the absorption-time trace to a homogeneous second-order function (Figure 1). However, under less acidic conditions when the $[\text{SCN}^-]$ was relatively low, first-order kinetics were observed. The first-order dependency on $[(\text{SCN})_2]$ under such conditions was confirmed by varying the $[(\text{SCN})_2]_0$ (Figure 2). The rate law does not depend upon the $[\text{SCN}^-]$ (Figure 3). Within the first-order regime, a slight

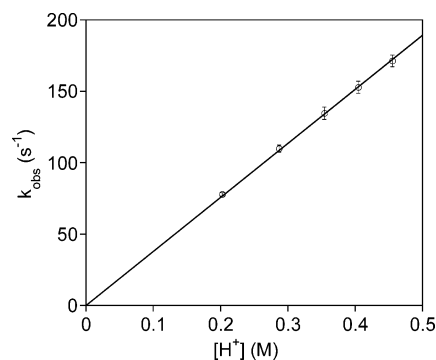


Figure 5. Observed pseudo-first-order rate constants for the comproportionation of HOSCN as a function of $[\text{H}^+]$. This measurement was achieved using a double-mixing stopped-flow sequence, where OSCN^- was generated in the first mixing cycle by the reaction of SCN^- and OBr^- at pH = 13 followed by a pH jump. Concentrations are for after the second mixing cycle: $[\text{SCN}^-] = 73.8$ mM; $[\text{OSCN}^-]_0 = 1.25$ mM; $I = 1.0$ M ($\text{NaClO}_4 + \text{HClO}_4 + \text{NaSCN}$); $[\text{H}^+] = 0.20\text{--}0.46$ M. The rate constant that is computed from these data is $k_{\text{comp}} = 5.14 (\pm 0.07) \times 10^3 \text{ M}^{-2} \text{ s}^{-1}$.

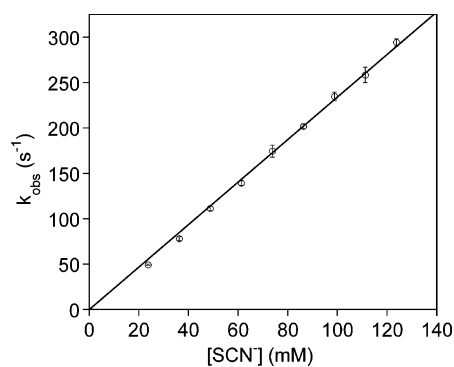


Figure 6. Observed pseudo-first-order rate constants for the comproportionation of HOSCN as a function of $[\text{SCN}^-]$. This measurement was achieved using the procedure that is described in the caption of Figure 4. Concentrations are for after the second mixing cycle: $[\text{H}^+] = 0.46$ M; $[\text{OSCN}^-]_0 = 1.25$ mM; $I = 1.0$ M ($\text{NaClO}_4 + \text{HClO}_4 + \text{NaSCN}$); $[\text{SCN}^-] = 23.8\text{--}123.8$ mM. The rate constant that is computed from these data is $k_{\text{comp}} = 5.15 (\pm 0.08) \times 10^3 \text{ M}^{-2} \text{ s}^{-1}$.

dependency on $[\text{H}^+]$ was observed for a given $[\text{SCN}^-]$, but the first-order rate constant appears to converge on a discrete value as the pH was raised (Table 1). There is an induction period at lower pH (e.g., Figure 2) which disappears at higher pH (e.g., Figure 4).

Kinetics of Comproportionation of Hypothiocyanous Acid and Thiocyanate. This reaction was investigated using a double-mixing stopped-flow sequence in which OSCN^- was generated in the first mixing cycle by oxidation of SCN^- with OBr^- and in the second mixing cycle a pH jump was induced.¹¹ In the presence of excess SCN^- and at constant pH, pseudo-first-order kinetics were observed. The observed pseudo-first-order rate constants exhibit first-order dependency on $[\text{H}^+]$ (Figure 5) and $[\text{SCN}^-]$ (Figure 6). Thus, the reaction exhibits overall third-order kinetics.

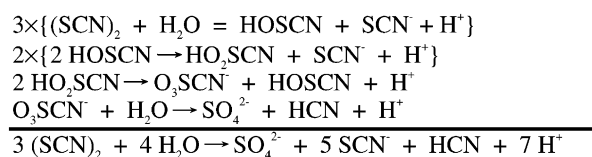
Discussion

Rate Law for Hydrolysis of Thiocyanogen. In deriving a rate law for the decomposition of $(\text{SCN})_2$, Stanbury et al. assumed HOSCN, $(\text{SCN})_2$, and $(\text{SCN})_3^-$ are in rapid equilibrium.⁹ Through $[\text{SCN}^-]$ -jump stopped-flow experiments, we have shown that the equilibrium between $(\text{SCN})_2$ and

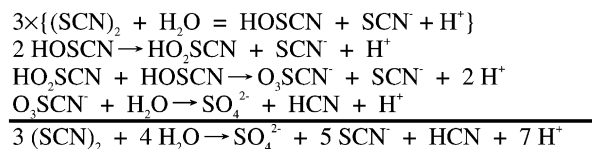
Comproportionation of HOSCN and SCN⁻

Scheme 1. Overall Stoichiometries of the Hydrolysis and Subsequent Disproportionation of (SCN)₂ for the Two Proposed Mechanisms

Mechanism I:

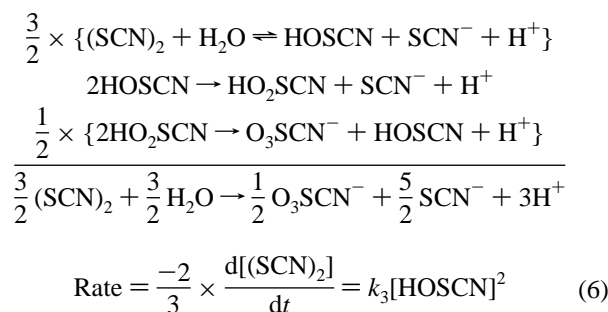


Mechanism II:



(SCN)₃⁻ occurs within the mixing time (unpublished results). However, the first-order kinetics we observed at low [H⁺] and [SCN⁻] suggest that hydrolysis can become rate-limiting under certain circumstances. Thus, in deriving our rate law we will assume that the equilibrium between (SCN)₂ and (SCN)₃⁻ is rapid, that the [HOSCN] achieves the steady-state, and that the disproportionation of HOSCN is rate-limiting. The mechanism that was previously proposed⁹ is illustrated as Mechanism I of Scheme 1. The rapid equilibrium between (SCN)₂ and (SCN)₃⁻ will be taken into consideration later. In addition to Mechanism I, Mechanism II is also conceivable (Scheme 1). The two mechanisms differ in the third step, namely disproportionation of HO₂SCN for the former mechanism and oxidation of HO₂SCN by HOSCN in the latter mechanism. We will derive a general rate law next, so that the reader may compare our results to those that have been previously reported by Stanbury et al.⁹ The derivation will also prove useful when we discuss the induction period that occurs at lower pH (e.g., Figure 2). Since neither our data nor that of Stanbury et al.⁹ are able to differentiate between these alternative reaction pathways, we consider both here, beginning with Mechanism I.

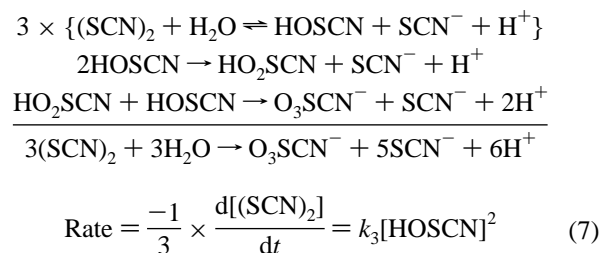
For Mechanism I, assuming that the disproportionation of HOSCN is rate-limiting and that the subsequent fast disproportionation of HO₂SCN yields an equivalent of HOSCN, we can define the rate in terms of the observable (SCN)₂ as:



where the rates in eq 6 are defined in terms of the elementary reactions above.²³

(23) The proportionality constants are defined for the elementary reaction (in some cases in curly brackets) using the convention for: $a\text{A} \rightarrow b\text{B}$; $-d[\text{A}]/(a \cdot dt) = d[\text{B}]/(b \cdot dt) = k[\text{A}]$.

For Mechanism II, assuming once more that the disproportionation of HOSCN is rate-limiting and that the subsequent fast reaction of HO₂SCN consumes an equivalent of HOSCN, we can define the rate as:



The two mechanisms differ in the definition of k_3 (the relationship between the definition of the rate in terms of the observable (SCN)₂ and the unobservable intermediate HOSCN). Since the next step of the derivation involves setting $d[\text{HOSCN}]/dt$ to zero, it does not matter whether its proportionality constant is 1/3 or 2/3. However, the proportionality constant with respect to (SCN)₂ does matter, in that it defines k_3 in terms of the observable. Since the present study does not differentiate between the two aforementioned mechanisms, we will define $k_3' = Pk_3$, where $P = 3/2$ and 3 for Mechanisms I and II, respectively. From this point forward, the derivation of the rate law is the same for the two mechanisms, beginning with the steady-state approximation:

$$\begin{aligned} \frac{-d[\text{HOSCN}]}{dt} &= k_3'[\text{HOSCN}]^2 + \\ &k_{-2}[\text{H}^+][\text{SCN}^-][\text{HOSCN}] - k_2[(\text{SCN})_2] = 0 \end{aligned} \quad (8)$$

$$\begin{aligned} [\text{HOSCN}]_{\text{SS}} &= \\ &\frac{-k_{-2}[\text{H}^+][\text{SCN}^-] \pm \sqrt{k_{-2}^2[\text{H}^+]^2[\text{SCN}^-]^2 + 4k_2k_3'[(\text{SCN})_2]}}{2k_3'} \end{aligned} \quad (9)$$

It is useful at this point to define a constant:

$$\text{Let } \alpha = \frac{4k_2k_3'}{k_{-2}^2[\text{H}^+]^2[\text{SCN}^-]^2} \quad (10)$$

which when incorporated into eq 9 yields:²⁴

$$[\text{HOSCN}]_{\text{SS}} = \frac{2k_2[(\text{SCN})_2]}{k_{-2}[\text{H}^+][\text{SCN}^-](\sqrt{1 + \alpha[(\text{SCN})_2]} + 1)} \quad (11)$$

Substituting [HOSCN]_{SS} into the rate law (eq 12) gives eq 13:

(24) Espenson, J. H. *Chemical Kinetics and Reaction Mechanisms*; McGraw-Hill: New York, 1981; pp 79–80.

$$\text{Rate} = \frac{-d[(\text{SCN})_2]}{dt} = k_3'[\text{HOSCN}]^2 \quad (12)$$

$$\frac{-d[(\text{SCN})_2]}{dt} = k_3' \times \left[\frac{2k_2[(\text{SCN})_2]}{k_{-2}[\text{H}^+][\text{SCN}^-] \left(\sqrt{1 + \frac{4k_2k_3'}{k_{-2}^2[\text{H}^+]^2[\text{SCN}^-]^2} [(\text{SCN})_2] + 1} \right)} \right]^2 \quad (13)$$

Equation 13 is useful for describing limiting extremes. If $1 \ll \alpha[(\text{SCN})_2]$ (which is expected to occur for high pH and low $[\text{SCN}^-]$), the k_2 step becomes rate-limiting, and first-order kinetics are expected:

$$\frac{-d[(\text{SCN})_2]}{dt} = k_3' \left[\frac{2k_2[(\text{SCN})_2]}{k_{-2}[\text{H}^+][\text{SCN}^-] \sqrt{\alpha[(\text{SCN})_2]}} \right]^2 = \frac{4K_2^2 k_3' [(\text{SCN})_2]}{\alpha[\text{H}^+]^2 [\text{SCN}^-]^2} = k_2 [(\text{SCN})_2] \quad (14)$$

In contrast, if $1 \gg \alpha[(\text{SCN})_2]$ (which can be expected for low pH and high $[\text{SCN}^-]$), the k_3 step becomes rate-limiting and second-order kinetics can be expected:

$$\frac{-d[(\text{SCN})_2]}{dt} = k_3' \left[\frac{k_2 [(\text{SCN})_2]}{k_{-2} [\text{H}^+][\text{SCN}^-]} \right]^2 = \frac{K_2^2 k_3' [(\text{SCN})_2]^2}{[\text{H}^+]_0^2 [\text{SCN}^-]_0^2} = k_{\text{eff}} [(\text{SCN})_2]^2 \quad (15)$$

Much of the data that were analyzed by Stanbury et al. exhibit clean second-order kinetics,⁹ although we conclude that some of the data at lower $[\text{H}^+]$ should be essentially first-order. In contrast, we have focused on the regime of $[\text{H}^+]$ and $[\text{SCN}^-]$ where the observed kinetics are essentially first-order. Accordingly, while the previously reported second-order kinetic data that were based upon changes in absorbance had to be converted to molar pseudo-second-order rate constants by applying a conversion factor,⁹ k_2 (the first-order rate constant for hydrolysis of $(\text{SCN})_2$) can be obtained directly from the spectral kinetic traces we have measured. Since the equilibrium between $(\text{SCN})_2$ and $(\text{SCN})_3^-$ is fast with respect to the rate of hydrolysis of $(\text{SCN})_2$ under the conditions that were employed during our measurements, the first-order decay of the absorbance (which is actually a composite of the absorption of $(\text{SCN})_2$ and $(\text{SCN})_3^-$) is proportional to $-d[(\text{SCN})_2]/dt$.

The data in Table 1 suggest that the observed first-order rate constants (k_{obs}) approach a pH-independent value of ca. 20 s^{-1} , which is consistent with the hydrolysis of $(\text{SCN})_2$ by H_2O (eq 2). This reaction can be considered to be a nucleophilic attack of H_2O on $(\text{SCN})_2$. A 7-orders-of-magnitude difference exists between the second-order rate constants for nucleophilic attack of H_2O versus OH^- on I_2 ,²⁵ so it is conceivable that the gradual increase of k_{obs} with

increasing pH that is evident in Table 1 is due to an increasing contribution of OH^- , even under the very acidic conditions of our measurements. There is a discernible induction period in the kinetic traces that are collected below ca. pH 2. We attribute this induction period to the formation of a steady-state concentration of HOSCN (eq 2). Thus, the kinetic traces illustrated in Figure 2, which were collected at pH 1.88, are best described by eq 13, which is somewhere between the limiting extremes of eqs 14 and 15. However, it is clear that the rate law that describes the kinetic traces in Figure 2 is much closer to eq 14 than eq 15. Thus, the traces after the induction periods are described well by a single exponential (Figure 2), the rate constants that are obtained when $[(\text{SCN})_2]_0$ is varied are essentially the same (Figure 2, $k_{\text{avg}} = 20.5 (\pm 1.6) \text{ s}^{-1}$), and the (pseudo)-first-order rate constants that are obtained when $[\text{SCN}^-]$ is varied are essentially the same (Figure 3, $k_{\text{avg}} = 19.7 (\pm 0.7) \text{ s}^{-1}$). The induction period disappears when the pH is greater than 2 and the resulting kinetics exhibit clean first-order behavior (Figure 4). When the $[\text{H}^+]$ is varied, the rate constant appears to converge on a value of ca. 20 s^{-1} (Table 1). Thus, the observed kinetics of hydrolysis is completely consistent with the model that has been employed to derive eq 13. Accordingly, these results suggest a fairly narrow window of $[\text{H}^+]$ and $[\text{SCN}^-]$ in which overall first-order behavior is observed.

It is noteworthy that an intermediate forms when I_2 reacts with H_2O that is best described as $\text{H}-\text{O}-\text{I}-\text{H}^+$ (vide infra). A corresponding intermediate forms when I_2 reacts with OH^- that is best described as $^- \text{I}-\text{I}-\text{OH}$ (vide infra). While we find it difficult to conceive of analogous intermediates for the reaction of H_2O and OH^- with $(\text{SCN})_2$, our measurements do not preclude the involvement of such species. In contrast to I_2 , no such adduct between H_2O or OH^- and X_2 ($\text{X} = \text{Cl}, \text{Br}$) has been detected in previous studies.^{26,27}

Rate Law for Comproportionation of Hypothiocyanous Acid and Thiocyanate. The rate law we employed for the determination of k_{-2} is more readily derived. Since under very acidic conditions the equilibrium of eq 2 lies far to the side of $(\text{SCN})_2$, the rate of approach to equilibrium beginning with HOSCN is effectively:

$$\text{Rate} = \frac{+d[(\text{SCN})_2]}{dt} = k_{-2}[\text{HOSCN}][\text{SCN}^-][\text{H}^+] \quad (16)$$

As expected, the rate of comproportionation of HOSCN and SCN^- exhibits overall third-order kinetics with first-order dependencies on $[\text{HOSCN}]$ (i.e., first-order kinetic traces in the presence of excess SCN^- and H^+), $[\text{H}^+]$ (Figure 5), and $[\text{SCN}^-]$ (Figure 6).

Equilibrium Constant for the Reversible Hydrolysis of Thiocyanogen. Stanbury et al. have taken two approaches to evaluating K_2 . In the first approach, the initial absorption at $\lambda = 300 \text{ nm}$ was fit to an equation that was derived using the assumption that the resulting absorption is the composite of the equilibria of eqs 1 and 2:⁶

(25) Lengyel, I.; Epstein, I. R.; Kustin, K. *Inorg. Chem.* **1993**, *32*, 5880–2.

(26) Beckwith, R. C.; Wang, T. X.; Margerum, D. W. *Inorg. Chem.* **1996**, *35*, 995–1000.

(27) Wang, T. X.; Margerum, D. W. *Inorg. Chem.* **1994**, *33*, 1050–5.

$$\epsilon_{\text{eff}} = \frac{\epsilon_{(\text{SCN})_2} + \epsilon_{(\text{SCN})_3^-} - K_1[\text{SCN}^-]}{1 + K_1[\text{SCN}^-] + \frac{K_2}{[\text{SCN}^-][\text{H}^+]}} \quad (17)$$

More recently, beginning with an equilibrium mixture of (SCN)₂ and (SCN)₃⁻, Stanbury et al. have investigated the reaction sequence of eqs 1–3.⁹ Their pseudo-second-order kinetic traces were fit to the rate law (where *P* was assigned a value of 3/2 by Stanbury et al.):⁹

$$\frac{-d[(\text{SCN})_2]}{dt} = P \times \left\{ \frac{K_2^2 k_3 [(\text{SCN})_2]^2}{[\text{H}^+]^2 [\text{SCN}^-]^2} + K_1 [(\text{SCN})_2]^3 [\text{H}^+]^2 + K_2 [\text{SCN}^-] [\text{H}^+] \right\} \quad (18)$$

The complexity of eq 18 (with respect to eq 15) stems from the fact that for constant [SCN⁻] and [H⁺] the observed rate data are pseudo-second-order (*k*_{obs}[']). Since homogeneous second-order kinetics depend upon the initial concentration of the reactant, *k*_{obs}['] must be written in terms of the partitioning between (SCN)₂ and (SCN)₃⁻ (i.e., by taking into account *K*₁):

$$k_{\text{obs}}' = P \times \frac{K_2^2 k_3}{[\text{H}^+]^2 [\text{SCN}^-]^2} \times \left(1 + K_1 [\text{SCN}^-] + \frac{K_2}{[\text{SCN}^-][\text{H}^+]} \right)^{-2} \quad (19)$$

In fitting their data to eq 19, *K*₁ was held constant (0.43 M⁻¹), and thus two parameters were obtained, *K*₂²*k*₃ and *K*₂. The value for *K*₂ that was obtained using eq 17 (*K*₂ = 5.4 (±1.9) × 10⁻⁴ M²) and the value that was obtained using eq 19 (*K*₂ = 5.66 (±0.77) × 10⁻⁴ M²) were self-consistent. By comparison, we obtained a value of *K*₂ = [HOXSCN]⁻ / [SCN⁻][H⁺] / [(SCN)₂] = *k*₂/*k*₋₂ = *k*_{hyd}^{SCN}/*k*_{comp}^{SCN} = 19.8 (±0.7) s⁻¹ / 5.14 (±0.07) × 10³ M⁻² s⁻¹ = 3.8 × 10⁻³ M², which differs from the values that were determined by Stanbury et al. by roughly an order of magnitude. However, given the potential sources of error (including a large estimated error for *K*₁ = 0.43 (±0.29) M⁻¹ and the likelihood that at least part of the data that were analyzed by Stanbury et al. were probably in the regime where eq 14 was more appropriate), we find the value of *K*₂ to be quite comparable to the value that was determined by largely independent means by Stanbury et al. This latter conclusion regarding the equilibrium constant of eq 2 adds credence to our conclusion that we have measured the rate constants of eq 2.

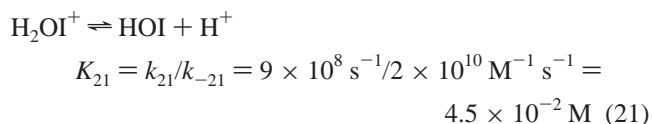
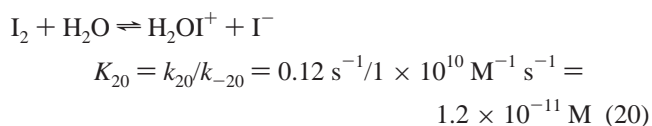
Comparisons with the Halogens. The rate constants for hydrolysis of the halogens (*k*_{hyd}^X) are compared with the rate constant for hydrolysis of (SCN)₂ (i.e., *k*₂) in Table 2. It is remarkable how similar *k*_{hyd}^X is for X = Cl, Br, and SCN (i.e., ca. 10–100 s⁻¹). In sharp contrast, *k*_{hyd}^I for I₂ is 5 orders of magnitude larger than the other (pseudo)halogens. Table 2 also summarizes the rate constants for comproportionation of HOX and X⁻ (*k*_{comp}^X), as well as the equilibrium constants that are derived from the ratio of the two rate

Table 2. Rate Constants for the Hydrolysis of X₂ (X₂ + H₂O), Rate Constants for Comproportionation of HOX and X⁻ (HOX + X⁻ + H⁺), and the Corresponding Equilibrium Constants

X	<i>k</i> _{hyd} ^X (s ⁻¹)	<i>k</i> _{comp} ^X (M ⁻² s ⁻¹)	<i>K</i> _{hyd} ^X = <i>k</i> _{hyd} ^X / <i>k</i> _{comp} ^X (M ²)	ref
Cl	15	1.8 × 10 ⁴	8.3 × 10 ⁻⁴	25 ^a
Br	98	1.6 × 10 ¹⁰	6.1 × 10 ⁻⁹	24 ^b
I	1.1 × 10 ⁸	2.0 × 10 ²⁰	5.4 × 10 ⁻¹³	23 ^c
SCN	20	5.1 × 10 ³	3.9 × 10 ⁻³	this study ^d

^a These data were determined at 20 °C and μ = 0.5 M. For comparison, *K*_{hyd}^{Cl} = 8.3 × 10⁻⁴ M² at 25 °C and μ = 0.1 M. ^b These data were determined at 25 °C and μ = 0.5 M. For comparison, *K*_{hyd}^{Br} = 6.2 × 10⁻⁹ M² at 25 °C and μ = 1.0 M. ^c Consult the discussion of eqs 20 and 21 herein and ref 23 for an explanation of the origin of these rate constants. ^d These data were determined at 18 °C, μ = 1.0 M.

constants, *K*_{hyd}^X = *k*_{hyd}^X/*k*_{comp}^X. Despite the fact that the redox potential of SCN⁻ lies somewhere between that of Br⁻ and I⁻,²⁸ the equilibrium constant for (SCN)₂ is more similar to Cl₂ than either Br₂ or I₂. Given that *k*_{hyd} is very similar for X = Cl, Br, and SCN, the similarity of *K* for X = Cl and SCN is due to their closely matched values of *k*_{comp}^X, which at ca. 10⁴ M⁻² s⁻¹ are substantially smaller than the corresponding values that have been determined for Br and I. Before continuing this discussion, it is important to note that the aqueous chemistry of I₂ and HOI is substantially more complicated than the corresponding chemistry for X = Cl, Br, and apparently for SCN. At high pH (above ca. pH 7), the major pathway of I₂ hydrolysis proceeds through nucleophilic attack that produces the intermediate I₂OH⁻. However, in the pH regime of this study (below pH 2), the major hydrolysis pathway for I₂ is via addition of H₂O and the intermediate H₂OI⁺. Thus, the equilibrium and rate constants for X = I in Table 2 are given by (*K*_{hyd}^I = *K*₂₀*K*₂₁):^{25,29,30}



Accordingly, the hydrolysis of I₂ is not an elementary reaction.

The hydrolysis of I₂ aside, it is apparent that the rates of hydrolysis of X₂ for X = Cl, Br, and SCN are comparable and that the differences between the positions of the equilibria lie in the relative rates of comproportionation. From a thermodynamic perspective, since HX are fully ionized, HOX are completely un-ionized, and the values of *k*_{hyd}^X are comparable, the trend of *k*_{comp}^{SCN} < *k*_{comp}^{Cl} ≪ *k*_{comp}^{Br} must relate to the relative stabilities of X₂ versus HOX and X⁻. These

(28) Hughes, M. N. General chemistry [of thiocyanic acid and its derivatives]. In *Chemistry and Biochemistry of Thiocyanic Acid Its Derivatives*; Academic Press: New York, 1975; pp 1–67.

(29) Sebok-Nagy, K.; Koertvelyesi, T. *Int. J. Chem. Kin.* **2004**, *36*, 596–602.

(30) Schmitz, G. *Int. J. Chem. Kin.* **2004**, *36*, 480–493.

relative stabilities are the result of a combination of bond enthalpies (e.g., X–X vs O–X) and solvation effects. Solvation energies are expected to be particularly important for the anions and for the species that can form strong hydrogen bonds. From a kinetic perspective, the trend that is observed for $k_{\text{hyd}}^{\text{X}}$ must reflect the relative nucleophilicity³¹ of X^- versus the electrophilicity of $\text{HO}^{\delta-}\text{X}^{\delta+}$. Regarding the nucleophilicity, we note that SCN^- is an ambidentate ligand and that it is known to produce products that are the result of both S and N nucleophilic attack.³² This naturally raises the question of whether the reactions we have studied involve HOSCN and/or HONCS. As noted earlier, we have previously investigated the structure of the initial product that is produced by the reaction of HOBr and SCN^- , the reaction we have employed herein to produce “HOSCN”, and we are convinced that the product is indeed HOSCN and not HONCS.¹² Thus, we are confident that we are measuring the rate of nucleophilic attack on HOSCN. Regarding the attacking nucleophile, the simplest mechanisms would be nucleophilic attack by the S of SCN^- . Since the Swain–Scott parameters suggest that Br^- and SCN^- are comparable nucleophiles and that both are better nucleophiles than Cl^- ($n = 2.99, 4.02,$ and 4.93 for Cl^- , Br^- , and SCN^- , respectively),³³ the origin of the trend in $k_{\text{hyd}}^{\text{X}}$ may be due to the relative electrophilicities of HOX. It is noteworthy that HOBr generally reacts several orders of magnitude faster with nucleophiles than HOCl does.^{34,35} Thus, HOBr appears to be the better electrophile. Unfortunately, there is a dearth of information regarding the reactivity of HOSCN, and in fact the comproportionation of HOSCN and SCN^- is the first reaction we are aware for which the rate has been measured. Fortunately, the corresponding rates of reaction of HOCl and HOBr with SCN^- are known. The second-order rate constants for the reaction of HOX with SCN^- are 2.3×10^7 ,

2.3×10^9 , and $5.1 \times 10^3 \text{ M}^{-1} \text{ s}^{-1}$ for $\text{X} = \text{Br}, \text{Cl},$ and SCN , respectively.^{10,11} Since these reactions involve a common reactant, we conclude that the relative electrophilicities are $\text{HOBr} > \text{HOCl} \gg \text{HOSCN}$, at least with respect to the nucleophile SCN^- . However, we note that the relative reactivities of HOCl and HOBr toward nucleophiles is largely independent of the nature of the nucleophile itself.^{34,35} It would appear likely that HOSCN is generally a relatively poor electrophile. Accordingly, it is not surprising that the only nucleophiles (other than SCN^-) that we have found that it reacts with are thiulates.³⁶ Since thiulates are very good nucleophiles, it is not surprising that they are among the most reactive species toward HOCl and HOBr as well.^{34,35}

Conclusion

We have measured the first-order rate constant for the hydrolysis of $(\text{SCN})_2$ by H_2O ($k_{\text{hyd}}^{\text{SCN}}$) and the corresponding third-order rate constant for the comproportionation of $\text{HOSCN} + \text{SCN}^- + \text{H}^+$ ($k_{\text{comp}}^{\text{SCN}}$). The values of $k_{\text{hyd}}^{\text{X}}$ for X_2 are within an order of magnitude for $\text{X} = \text{Cl}, \text{Br},$ and SCN . In contrast, while the values of $k_{\text{comp}}^{\text{X}}$ are comparable for $\text{HOX} + \text{X}^- + \text{H}^+$ for $\text{X} = \text{Cl}$ and SCN , $k_{\text{comp}}^{\text{Br}}$ for $\text{X} = \text{Br}$ is 6 orders of magnitude larger. We propose that the mechanism of comproportionation involves nucleophilic attack on HOX by X^- . While the relative nucleophilicities of X^- are $\text{SCN}^- > \text{Br}^- \gg \text{Cl}^-$, the electrophilicities of HOX are $\text{HOBr} > \text{HOCl} \gg \text{HOSCN}$. In addition to explaining the trend in $k_{\text{comp}}^{\text{X}}$, the ordering of nucleophilicities and electrophilicities rationalize the trend in the reactions of HOX with SCN^- : $\text{HOBr} > \text{HOCl} \gg \text{HOSCN}$.

Acknowledgment. We appreciate the National Science Foundation (CHE-0503984), the American Heart Association (0555677Z), and the Petroleum Research Fund (42850-AC4) for their financial support. We are also grateful to reviewers of this manuscript who provided insightful comments.

IC061470I

(31) Phan, T. B.; Breugst, M.; Mayr, H. *Angew. Chem., Int. Ed.* **2006**, *45*, 3869–3874.

(32) Loos, R.; Kobayashi, S.; Mayr, H. *J. Am. Chem. Soc.* **2003**, *125*, 14126–14132.

(33) Koskikallio, J. *Acta Chem. Scand.* **1969**, *23*, 1477–89.

(34) Pattison, D. I.; Davies, M. J. *Chem. Res. Toxicol.* **2001**, *14*, 1453–64.

(35) Pattison, D. I.; Davies, M. J. *Biochem.* **2004**, *43*, 4799–4809.

(36) Ashby, M. T.; Aneetha, H. *J. Am. Chem. Soc.* **2004**, *126*, 10216–10217.